ELSEVIER

NeuroImage

www.elsevier.com/locate/ynimg
NeuroImage 22 (2004) 394–400

Regional homogeneity approach to fMRI data analysis

Yufeng Zang,[a] Tianzi Jiang,[a,b,*] Yingli Lu,[a] Yong He,[a] and Lixia Tian[a]

[a] *National Laboratory of Pattern Recognition, Institute of Automation, Chinese Academy of Sciences, Beijing 100080, PR China*
[b] *Key Laboratory of Mental Health, Chinese Academy of Sciences, Beijing 100101, PR China*

Received 16 October 2003; revised 18 December 2003; accepted 18 December 2003

Kendall's coefficient concordance (KCC) can measure the similarity of a number of time series. It has been used for purifying a given cluster in functional MRI (fMRI). In the present study, a new method was developed based on the regional homogeneity (ReHo), in which KCC was used to measure the similarity of the time series of a given voxel to those of its nearest neighbors in a voxel-wise way. Six healthy subjects performed left and right finger movement tasks in event-related design; five of them were additionally scanned in a rest condition. KCC was compared among the three conditions (left finger movement, right finger movement, and the rest). Results show that bilateral primary motor cortex (M1) had higher KCC in either left or right finger movement condition than in rest condition. Contrary to prediction and to activation pattern, KCC of ipsilateral M1 is significantly higher than contralateral M1 in unilateral finger movement conditions. These results support the previous electrophysiologic findings of increasing ipsilateral M1 excitation during unilateral movement. ReHo can consider as a complementary method to model-driven method, and it could help reveal the complexity of the human brain function. More work is needed to understand the neural mechanism underlying ReHo.

Keywords: fMRI; Kendall's coefficient concordance; Motor cortex; General linear model

Introduction

Deoxyhemoglobin in venous blood is a natural contrast agent, which underlies functional MRI (fMRI) in vivo brain (Ogawa et al., 1990). Task-related hemodynamic response is taken as the basis of many analytical techniques. Some simple and effective model-driven methods were developed at the early stage of fMRI (Bandettini et al., 1993; Friston, 1996). Model-driven methods are based on a priori models; for example, a square wave or its convolution with hemodynamic response function (HRF), as typically implemented in the Statistical Parametric Mapping (SPM) (Friston, 1996). One problem with model-driven analysis is that hemodynamic response may vary from region to region (Moritz et al., 2000) and even from trial to trial (Duann et al., 2002; Richter et al., 1997). General linear model with deconvolution (GLM-De) method (see Cox, 1996; in section Deconvolution Analysis of fMRI Time Series Data by B. Douglas Ward in AFNI. Version 2.12c) allows HRF to vary from voxel to voxel. However, it also takes variability across trials as noise. In spite of these shortcomings, these model-driven methods are still very popular among researchers due to their easy implementation and physiologically meaningful a priori hypothesis.

Many data-driven methods have also been developed. Some typical examples include clustering analysis (Baumgartner et al., 1997; Filzmoser et al., 1999), principal component analysis (PCA) (Hansen et al., 1999; Lai and Fang, 1999), independent component analysis (ICA) (Calhoun et al., 2001; Duann et al., 2002; McKeown et al., 1998), and self-organizing maps (SOMs) (Ngan and Hu, 1999). Without any a priori assumption on hemodynamic model, data-driven methods can gather more information than model-driven ones. Powers of data-driven methods are that they can identify nonanticipated or transient task-related components. However, there exist some inherent drawbacks with the above-mentioned data-driven methods. For instance, clustering methods have to face the "cluster validity" problem; PCA needs orthogonal patterns assumption, and ICA needs statistically independent assumption. Moreover, few studies have compared data-driven method with the popular model-driven method, GLM-De, at group-subjects level.

Clusters identified with most data-driven methods have no information of how good the intracluster homogeneity is (Goutte et al., 1999). Even if for the clusters identified with model-driven methods, time courses highly correlated with the model may not correlate well with each other (Baumgartner et al., 1999). Baumgartner et al. (1999) used Kendall's coefficient of concordance (KCC) for purification of the activated clusters. Based on their purification work and our previous region growing method (Lu et al., in press), we here propose a regional homogeneity (ReHo) method. Similar to our region growing method, ReHo assumes that a given voxel is temporally similar to that of its neighbors. We also hypothesize that ReHo could be modulated in pertinent cognitive tasks. KCC (Kendall and Gibbons, 1990) was used to measure ReHo of the time series of a given voxel with those of its nearest neighbors in a voxel-wise way. Then, the KCC value was given to this voxel, and individual KCC map was obtained. Considering that either the magnitude used for spatial smoothing during preprocess-

* Corresponding author. National Laboratory of Pattern Recognition, Institute of Automation, Chinese Academy of Sciences, Beijing 100080, PR China. Fax: +86-10-62551993.
E-mail addresses: yfzang@nlpr.ia.ac.cn (Y. Zang), jiangtz@nlpr.ia.ac.cn (T. Jiang), yllu@nlpr.ia.ac.cn (Y. Lu).
Available online on ScienceDirect (www.sciencedirect.com.)

1053-8119/$ - see front matter © 2004 Elsevier Inc. All rights reserved.
doi:10.1016/j.neuroimage.2003.12.030

ing stage or the size of cluster to be measured might affect KCC value, we used three sorts of spatial smoothing (0, 4, and 8 mm, respectively; see Data preprocessing in Materials and methods) and three sorts of cluster size (7, 19, and 27 voxels, respectively. See Regional homogeneity in Materials and methods). A second-level statistical analysis was used to draw inference from population. The statistical results of ReHo were compared with a typical model-driven method, GLM-De (Cox, 1996; Version 2.52c).

Materials and methods

Subjects

Six right-handed subjects (aged 23–40 years; mean, 23.7 years; two males and four females) served as subjects. Normal or corrected-to-normal vision and no history of neurologic and psychiatric disorder were needed. Informed written consent was obtained from all subjects. The experiments were approved by the Research Board of Institute of Automation, Chinese Academy of Sciences.

Tasks

Six subjects performed a finger movement task. Five of them (four females and one male) had additional scanning session in a rest condition before movement task. During the rest condition session, subjects were instructed to close their eyes and to not think of anything particular. This session lasted 7 min. The finger movement task was generated in PC by free software PRESENTATION (http://www.neurobehavioralsystems.com) and was projected to the mirror above subjects via a video projecting system. The visual angle was 5°. The background was white, and the foreground was black. A vertical line existed as fixation stimulus at the center of the screen all along the movement task scanning session. At the beginning of each trial, a circle flashed at a frequency of 2 Hz for four times on the left or right to the fixation line in pseudorandom order. There was a key box in each of left and right hand of the subject. The subject was instructed to press the key with left or right thumb for four times, corresponding to the left or right stimuli, respectively, as soon as the flashing circle disappeared. After finger movement, the subjects were instructed to keep stationary and to keep attention to the onset of next stimulus. This period lasted 10–18 s in a pseudorandom way across trials. There were totally 28 trials during the finger movement scanning session, 14 for left hand and 14 for right hand. The finger movement scanning session lasted 7 min. Investigators in the operating room could visually monitor the subjects' responses, and no behavioral error was found. Before scanning, each subject had practiced the tasks.

Scanning procedures

Scans were acquired on a SIEMENS TRIO 3-Tesla scanner in the Institute of Biophysics, Chinese Academy of Sciences. Subjects lay supine in the scanner, and their head was snugly fixed with foam pads and a belt. For each resting and finger movement scanning session, 32 axial slices with echo-planar images (EPI) pulse sequence (thickness/gap = 3.0/0.75 mm, in-plane resolution = 64 × 64, TR = 2000 ms, TE = 30 ms, flip angle = 90°, FOV = 220 × 220 mm), and 210 volumes were obtained. At the same position, 32 slices by spin echo sequence (thickness/gap = 3.0/0.75 mm, in-plane resolution = 256 × 256, FOV = 200 × 200 mm, TR = 4000 ms, TE = 29 ms) were acquired. Finally, 192 T1 sagittal images (TR = 1730 ms, TE = 3.93 ms, thickness = 1.0 mm, no gap, in-plane resolution = 256 × 256, FOV = 240 × 240 mm, flip angle = 15°) covering the whole brain were obtained.

Data preprocessing

We used AFNI (Cox, 1996; Version 2.52c) for preprocessing and GLM-De analysis. For the rest condition data, the first 10 time points were discarded for scanner calibration and for subjects to get used to the circumstance. Redundant (relative to finger movement conditions) 122 time points of the latter part were also discarded. Thus, 78 time points from the rest condition time series were kept for ReHo analysis (see Regional homogeneity section). For finger movement data, the first two trials (28 time points) were discarded. Thus, 192 time points, 13 trials for each of left and right hand, were kept. No visible head movement was found by cinematic viewing at EPI images of all subjects. Further preprocessing procedures included motion correction, within-subject registration, time aligning across slices, time series linear detrending, voxels resampling to 3 × 3 × 3 mm^3, spatially smoothing [FWHM = 0 (i.e., no spatially smoothing), 4, and 8 mm, respectively] and spatially normalizing (Talairach and Tournoux, 1988). Individual mask was created from the three-dimensional data by setting the value of voxels out of brain to zero by Brain Extraction Tool (Smith, 2002). After averaging all the individual masks, any voxel's value would be set to zero if this voxel was not scanned from all six subjects. For the data of either finger movement conditions or rest conditions, only the voxels within the averaged mask was taken into further analysis.

GLM with deconvolution

Individual activation maps were generated by deconvolution program in AFNI (Cox, 1996; Version 2.12c, section *Deconvolution Analysis of fMRI Time Series Data* by B. Douglas Ward) voxel by voxel. First, the impulse response functions (IRF) were estimated based on the input stimulus functions and the observed fMRI time series. The impulse response functions were then convolved with the stimulus functions to yield the estimated response. Finally, the F statistics was calculated for each voxel to test the "goodness" of the fit between the observed time series and the estimated response. Selected parameters are minimum lag = 0, maximum lag = 5, that is, hemodynamic response duration being assumed to be six time points (12 s). The individual F maps for left and right finger movement conditions were converted to normal distribution Z maps. Individual IRFs for each left and right finger movement task were also obtained from GLM-De.

Regional homogeneity

As described above, the length of IRF for each trial of finger movement was assumed to be six time points (12 s). Then, 13 trials, totally 78 time points, were picked out, and new time series was acquired for each left and right finger movement conditions. The rest condition data also consisted 78 time points. Thus, three new kinds of time series were obtained for five subjects. The other subject had only two new kinds of movement time series. All the

Table 1
The number of masses (MN) showing significant difference and the total number of voxels (TV, in mm^3) meeting the given criteria

FWHM	KCC						*Z*	
	7		19		27		MN	TV
	MN	TV	MN	TV	MN	TV		
0	1	1259	7	9054	8	11,573	1	2349
4	5	8536	8	12,312	22	32,914	14	19,683
8	18	31,874	22	46,457	28	59,152	27	117,450

FWHM: 0 (no spatial smoothing), 4, and 8 mm, respectively. Value under KCC: cluster size = 7, 19, and 27 voxels, respectively. *Z*: *t* test results from *Z* maps of GLM-De.

new time series were taken into ReHo calculation. A KCC (Kendall and Gibbons, 1990) was assigned to a given voxel by calculating the KCC of time series of this voxel with those of its nearest neighbors (6, 18, and 26, respectively):

$$W = \frac{\Sigma(R_i)^2 - n(\overline{R})^2}{\frac{1}{12}K^2(n^3 - n)} \quad (1)$$

where W is the KCC among given voxels, ranged from 0 to 1; R_i is the sum rank of the ith time point; where $\overline{R} = ((n+1)K)/2$ is the mean of the R_i's; K is the number of time series within a measured cluster (here, $K = 7$, 19, and 27, respectively; one given voxel plus the number of its neighbors); n is the number of ranks (here $n = 78$). The KCC program was coded in MATLAB (The MathWorks, Inc., Natick, MA). Thus, an individual ReHo map was generated for each dataset.

Paired t test statistical inference

As Fig. 1 shows, it is more difficult to get direct meaningful results from individual KCC maps than from *Z* maps, although higher KCC could be seen at ipsilateral primary motor cortex (M1) than contralateral M1 (Figs. 1c and d). Hence, paired *t* test was done to compare different conditions. Such paired *t* test is a second-level analysis corresponding to random effects across subject, which has been performed elsewhere (e.g., Doyon et al., 2002; Greicius et al., 2003). For left and right finger movement conditions, six subjects were included. Paired *t* test was done between the two groups on *Z* maps obtained by GLM-De method and on KCC maps obtained by ReHo method, respectively. Voxel's *t* value of >2.571 ($P < 0.05$; $n = 6$) and mass volume of >540 mm^3 were considered as significantly different between left and right hand movement conditions. There were totally nine parameter combinations for ReHo: three sorts of spatial smoothing multiplying three sorts of cluster size. However, for GLM-De, there were only three sorts of spatial smoothing. Therefore, 12 paired *t* tests were done to get difference between left and right finger movements. The number of masses and the total number of voxels above the given threshold were illustrated

Table 2
Detailed information about difference between left and right finger movements by methods ReHo (magnitude of spatial smoothing FWHM = 4 mm and size of cluster = 27 voxels) and GLM-De (magnitude of spatial smoothing FWHM = 4 mm)

KCC						*Z*					
MV	*x*	*y*	*z*		Location, BA	MV	*x*	*y*	*z*		Location, BA
9084	32.1	−20	56.6	R	M1, 4	8883	38.2	−24.1	52.6	R	M1, 4
3748	3.6	−53.8	19.3	R	PCC, 23, 30	1512	−40	−21.2	49.8	L	M1, 4
2161	0.7	49.3	20.2	B	MdFG, 9	1215	12.1	−17.5	10.7	R	Tha
1778	0.8	45.2	−4.4	B	MdFG, 32	1161	3.7	0.1	42.9	R	SMA, 6
1477	−52.9	−6.2	−5.1	L	STG, 21	972	−23.9	−62.7	44.4	L	PPC, 7
1341	−31.5	41.6	14.2	L	MiFG, 46	810	−36.7	−49.5	49.2	L	SPL, 7
1149	35.6	−60.3	−18.7	R	FG, 37	783	8.7	−40	67.5	R	PCL, 5
1122	−45.3	−61.2	26.5	L	AG, 39	729	45.6	−32.4	−13.7	R	MiTG, 22
1122	−40.7	−22.4	52.8	L	M1, 4	675	50.9	−13.1	13.8	R	TTG, 42
1067	−12.3	−4.8	10.3	L	Tha	675	12.3	−17.3	67.7	R	MdFG, 6
1040	28.2	34.8	−5.7	R	IFG, 47	594	−49.1	−36.9	18	L	STG, 22
985	−16.6	−81.6	−1.7	L	LG, 18	567	43.5	−66.6	−1.1	R	ITG, 19
848	6.1	−39.6	65.7	R	PCL, 5	567	3.7	−77.8	36.5	R	PCu, 7
821	−26.8	23.6	47.7	L	MiFG, 8	540	22.7	−66.8	8.8	R	LG, 18
766	−50.4	−27.4	3.8	L	STG, 22						
711	5.3	−19.4	48.7	R	SMA, 6						
684	50.3	8.9	−13.5	R	STG, 38						
657	−32.6	−40.1	35.6	L	SMG, 40						
629	−32.4	−6.1	−25.6	L	PHG, 35						
602	39.5	−51	−0.7	R	MiTG, 21						
575	25.8	−48.3	63.2	R	SPL, 7						
547	9.5	−67.1	−19	R	Cerebellum						

Left part: results based on KCC maps from ReHo. Right part: results based on *Z* maps from GLM-De. MV denotes mass volume (in mm^3); *x*, *y*, *z*, coordinates (in mm^3) of the mass center in normalized atlas; BA, Broadmann area; L, left; R, right; B, bilateral.
Nomenclature abbreviations. AG denotes angular gyrus; FG, fusiform gyrus; IFG, inferior frontal gyrus; ITG, inferior temporal gyrus; LG, lingual gyrus; PCL, paracentral lobulus; M1, primary motor cortex; MdFG, medial frontal gyrus; MiFG, middle frontal gyrus; MiTG, middle temporal gyrus; PCC, posterior cingulate cortex; PCu, precuneus; PHG, parahippocampal gyrus; PPC, posterior parietal cortex; SMA, supplementary motor area; SMG, supramarginal gyrus; SPL, superior parietal lobulus; STG, superior temporal gyrus; Tha, thalamus; TTG, transversal temporal gyrus.

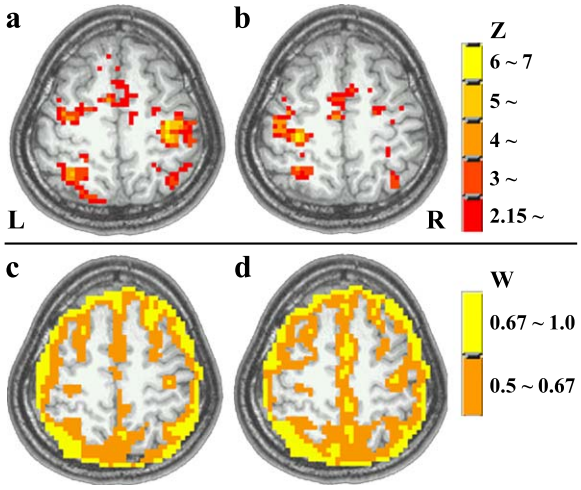

Fig. 1. The *Z* maps (a, b, with spatial smoothing FWHM = 4 mm) and KCC maps (c, d, with parameters combination of spatial smoothing FWHM = 4 mm and cluster size = 27 voxels) from the selected subject. (a, c) Left finger movement. (b, d) Right finger movement. L denotes left; R, right. Note that the threshold 0.5 of KCC (W) is an arbitrary value between 0 and 1.

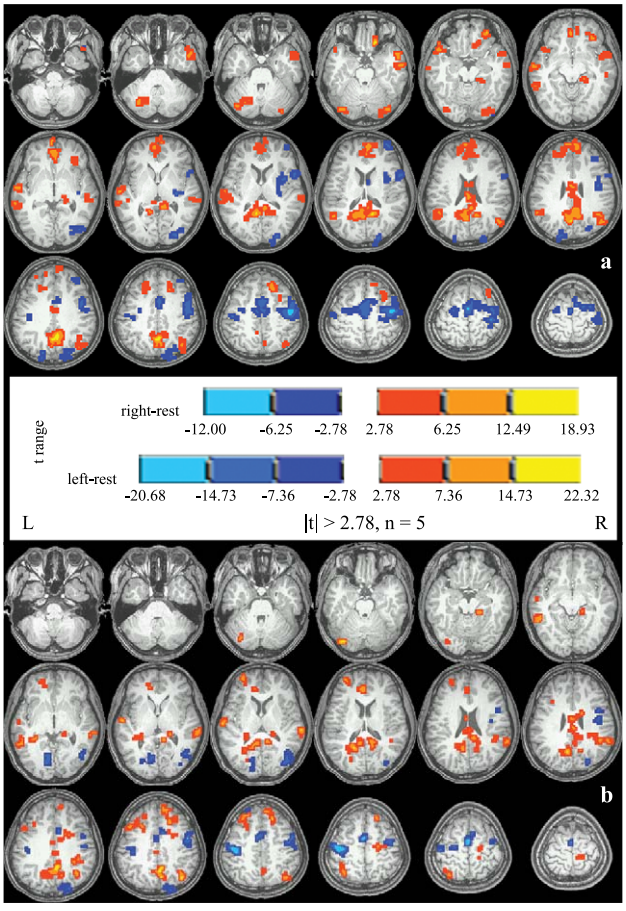

Fig. 4. Paired *t* test on KCC value between movement condition and rest condition. (a) Right finger movement versus rest. (b) Left finger movement versus rest. Dark color: hand movement > rest; bright color: rest > hand movement. L denotes left; R, right.

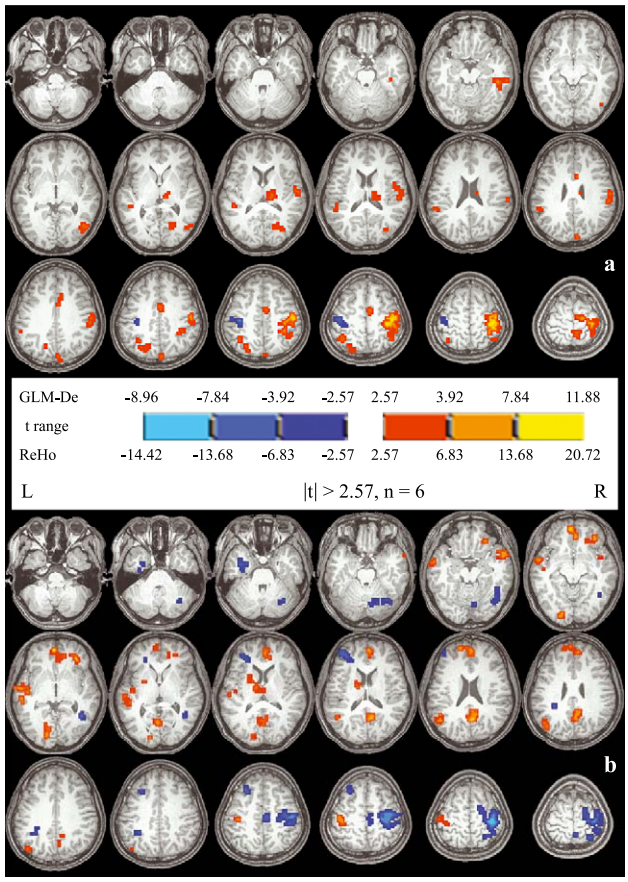

Fig. 3. Paired *t* test between left and right hand movement conditions based on *Z* maps (with FWHM = 4 mm) by GLM-De (a) and KCC maps (with FWHM = 4 mm and cluster size = 27 voxels) by ReHo (b). Bright color: left hand > right hand; dark color: right hand > left hand. L denotes left; R, right.

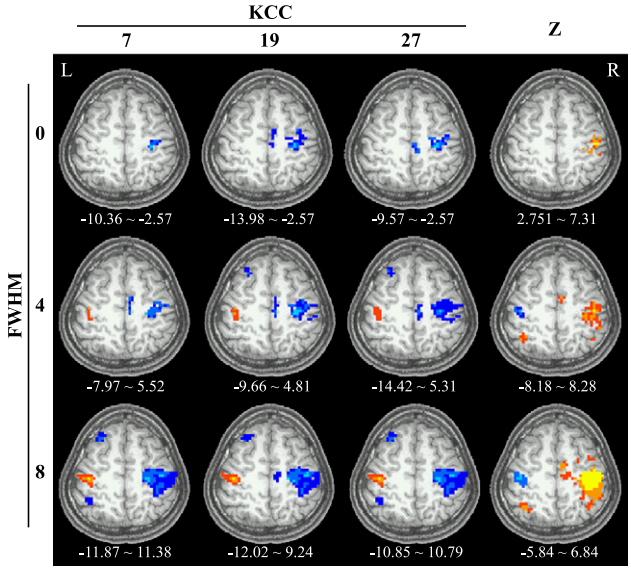

Fig. 2. Results from the 12 paired *t* tests in one slice (*z* coordinate = 52 mm in normalized atlas). From top to bottom: FWHM = 0, 4, and 8 mm, respectively. From left to right under KCC cluster size = 7, 19, and 27 voxels, respectively. *Z* denotes results of *t* test on *Z* maps of GLM-De. Values under each figure are *t* range of the *t* test. Note that $t > 2.571$. L denotes left; R, right.

in Table 1. For display purposes, results from the 12 paired *t* tests in one slice (*z* coordinate = 52 mm in normalized atlas) including M1 and supplementary motor area (SMA) were presented in Fig. 2.

For detailed information about difference between left and right finger movements by ReHo and GLM-De methods, a parameter of FWHM = 4 mm was selected for both method, and 27 voxels for cluster size were chosen for ReHo. Choosing these parameters was a bit arbitrary, because it was unknown which voxels are true positive or true negative by the paired *t* test. Detailed information, including mass size, location of mass center, and so on, was illustrated in Table 2.

For rest condition, only five subjects were included. Only one parameter combination (FWHM = 4 mm and cluster size = 27 voxels) was used. Paired *t* test was done between left hand movement condition and rest condition (left vs. rest), and similarly, between right hand movement condition and rest condition (right vs. rest). Voxel's *t* value of >2.776 ($P < 0.05$; $n = 5$) and mass volume of >540 mm^3 were considered as significantly different between movement and rest conditions.

As small number of subjects was included in this study, correction for multiple comparisons was done neither across whole brain voxels nor across the three conditions.

At bilateral M1, voxels with greatest *t* value obtained by paired *t* test on *Z* maps (spatial smoothing magnitude FWHM = 4 mm) were taken as peak voxels. These peak voxels' *Z* value of movement conditions and their KCC value (spatial smoothing magnitude FWHM = 4 mm and cluster size = 27 voxels) in the three conditions (two movement conditions and one rest condition) were illustrated in Fig. 5. The peak voxels' IRFs from one selected subject were also illustrated.

Results

Effects of magnitude of spatial smoothing and size of cluster on KCC

From Table 1, one can see that the magnitude of spatial smoothing affects the results of either ReHo or GLM-De; that is, large magnitude of spatial smoothing yielded more significant difference between left and right finger movements. The size of cluster (7, 19, or 27 voxels) to be measured had strong effect on KCC; that is, large size yielded much difference between the two tasks. However, for merely M1 and SMA (Fig. 2), the size of cluster does not seem to significantly affect the difference between the two tasks.

Paired t test on Z maps (Fig. 3a and Table 2)

As expected, contralateral M1 was more strongly activated than ipsilateral one during unilateral finger movement. Compared between left and right finger movements, left finger movement activated larger mass volume in right M1 than right finger movement did in left M1. Stronger activation by left finger movement could also be seen in right supplementary motor area (SMA), right thalamus, left posterior parietal cortex [Broadmann area (BA) 7], and so on. Except for left M1, no other brain area was

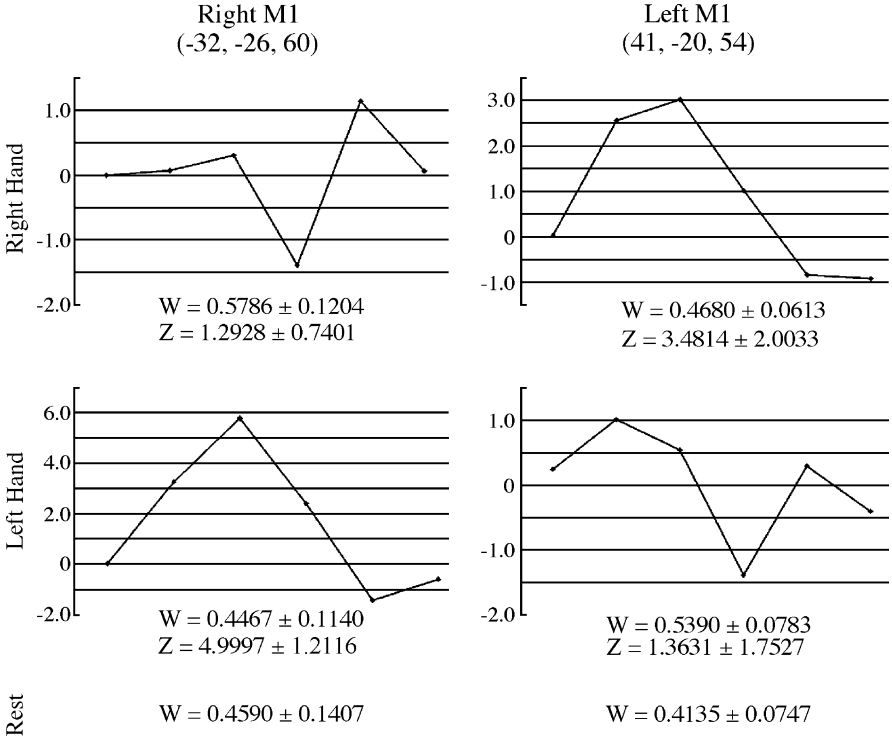

Fig. 5. Mean and standard deviation of *Z* value, KCC value (W) and IRF of the peak voxels at bilateral M1 (see Materials and methods). The IRFs are from the selected subject. The value on *y*-axis of IRF is the regression coefficient at a given time point (totally, in the current study, six time points, corresponding to 12 s).

found more strongly activated by right finger movement than left one at the given threshold (Fig. 3a and Table 2).

Paired t test on KCC maps (Figs. 2 and 3b, and Table 2)

Very interestingly, results from paired *t* test on KCC maps between left and right finger movement conditions seemed to be contrary to that from GLM-De. KCC value in ipsilateral M1 during unilateral finger movement was higher than in contralateral M1. Moreover, right finger movement induced larger mass volume in right M1 than left finger movement did in left M1. Such higher KCC in ipsilateral M1 could be seen by any parameter combination (Fig. 2). Besides right M1, higher KCC by right than left finger movement could be seen in right SMA, left middle frontal gyrus (BA 8), left posterior parietal cortex (BA 7) and so on. Besides left M1, higher KCC by left than right hand finger movement could be seen at left thalamus, bilateral medial frontal gyri (BA 10 and 32), bilateral posterior cingulate cortices (PCC; BA 23 and 30), left middle temporal gyrus (BA 22), and so on.

KCC of bilateral M1 and bilateral SMA was higher in either left or right finger movement condition than in rest condition (Figs. 4 and 5). Higher KCC in rest condition than in left or right finger movement conditions could be seen at bilateral medial frontal gyri (BA 9 and 32) and PCC, and so on.

IRF, Z value and KCC value in bilateral M1

Fig. 5 shows that IRF in contralateral M1 is much "better" than that from ipsilateral M1 in unilateral finger movement. Accordingly, larger *Z* value indicates less variability of the IRF from trial to trial in contralateral M1. KCC in ipsilateral M1 is higher than that in contralateral M1 during unilateral finger movement. KCC in bilateral M1 is higher in movement conditions than in rest condition.

Discussions

In this study, results with GLM-De show that contralateral M1 is more significantly activated with unilateral finger movement than ipsilateral M1. However, the results of ReHo seem, to some extent, contrary to that by GLM-De; that is, KCC of ipsilateral M1 is higher than that of contralateral M1.

Electrophysiologic studies (Salmelin et al., 1995; Urbano et al., 1998; Ziemann and Hallett, 2001) have shown that ipsilateral M1 is also activated during ipsilateral hand movement. The neural basis of such ipsilateral activation remains unclear. Due to the nature that fMRI signal is a relative hemodynamic change, some results from fMRI studies on ipsilateral M1 activation have been quite inconsistent to each other. For example, some results showed activation, that is, increased hemodynamic response (Bernard et al., 2002; Cramer et al., 1999) in ipsilateral M1 while some showed deactivation, that is, decreased hemodynamic response (Allison et al., 2000; Hamzei et al., 2002) during ipsilateral hand movements. In this study, activation by GLM-De showed no much difference between left and right M1 in ipsilateral movement condition (see *Z* value in Fig. 5; right-hand−right-M1 vs. left-hand−left-M1 = 1.2928 ± 0.7401 vs. 1.3631 ± 1.7527). This result by GLM-De does not support previous fMRI findings of activation or deactivation in ipsilateral M1. However, the KCC of ipsilateral M1 is significantly higher than contralateral M1. This result partly supports ipsilateral activation found by electrophysiologic studies. GLM-De is a model-driven method. It requires a hypothesis that there should be event-related hemodynamic response and that the hemodynamic response is constant across events (trials or stimuli). With so many constraints, GLM-De might not have demonstrated hemodynamic changes in ipsilateral M1 during unilateral hand movement. However, the data-driven method ReHo has no any a priori stimulus−response model. We believe that changed KCC implies changed hemodynamic response, but the character of such hemodynamic response needs to be further investigated in future.

Another interesting finding in the present study is higher KCC in PCC in rest condition than in movement conditions. A few studies have revealed a network of cortical areas, including PCC, activated during conscious rest state as compared to other cognitive states (Mazoyer et al., 2001; Raichle et al., 1997; Shulman et al., 1997). PCC has been considered as a critical node in this network (Greicius et al., 2003). The presented ReHo method successfully detected PCC in resting state as compared to finger movement conditions.

Some parameters can significantly affect the results of ReHo. The current results show that the magnitude of spatial smoothing affects the result of either ReHo or GLM-De; that is, larger magnitude of spatial smoothing yielded more significant difference between left and right finger movements. The size of cluster (7, 19, or 27 voxels, respectively) to be measured had strong effect on KCC; that is, larger size yielded more difference between the two tasks. Similarly, the magnitude of spatial smoothing also significantly affects the result of GLM-De. Although it seems difficult to optimize these parameters from the current study, higher KCC in ipsilateral M1 was confirmed by any parameter combination (Fig. 2). Moreover, this result is consistent to previous electrophysiologic findings (Salmelin et al., 1995; Urbano et al., 1998; Ziemann and Hallett, 2001). Compared to GLM-De, ReHo is not efficient to detect changes in contralateral M1. Therefore, ReHo and GLM-De should be complementary to each other.

In addition to the parameters like magnitude of spatial smoothing and cluster size to be measured, other factors, for example, the volume of a specific brain area to be studied, might also affect the results. It should also be noted that ReHo method could be used for blocked design, slow event-related design, and the resting state. However, it is not suitable for rapid event-related design, because the hemodynamic response of more than one kind of tasks overlapped on each other.

In summary, ReHo supposed that voxels within a functional brain area were more temporally homogeneous when this area is involved in a specific condition. Compared to model-driven method like GLM-De, ReHo seems to be less sensitive to constant event-related hemodynamic responses. However, its major advantage is the ability to detect unpredicted hemodynamic responses that model-driven method failed to find out. Such unpredicted hemodynamic responses could help us understand the high complexity of the human brain function.

Acknowledgments

The authors are highly grateful to the anonymous referees for their significant and constructive critiques and suggestions, which improve the paper very much. This work was partially supported by Hundred Talents Programs of the Chinese Academy of Sciences,

the Natural Science Foundation of China, Grant No. 60172056, 60121302, and 30270444, and the National Key Basic Research and Development Program (973) Grant No. 2003CB716104.

References

Allison, J.D., Meador, K.J., Loring, D.W., Figueroa, R.E., Wright, J.C., 2000. Functional MRI cerebral activation and deactivation during finger movement. Neurology 11, 135–142.

Bandettini, P.A., Jesmanowicz, A.J., Wong, E.C., Hyde, J.S., 1993. Processing strategies for time-course data sets in functional MRI of the human brain. Magn. Reson. Med. 30, 161–173.

Baumgartner, R., Scarth, G., Teichtmeister, C., Somorjai, R., Moser, E., 1997. Fuzzy clustering of gradient-echo functional MRI in the human visual cortex: Part I. Reproducibility. J. Magn. Reson. Imaging 7, 1094–1101.

Baumgartner, R., Somorjai, R., Summers, R., Richter, W., 1999. Assessment of cluster homogeneity in fMRI data using Kendall's coefficient of concordance. Magn. Reson. Imaging 17, 1525–1532.

Bernard, R.A., Goran, D.A., Sakai, S.T., Carr, T.H., McFarlane, D., Nordell, B., Cooper, T.G., Potchen, E.J., 2002. Cortical activation during rhythmic hand movements performed under three types of control: an fMRI study. Cogn. Affect. Behav. Neurosci. 2, 271–281.

Calhoun, V.D., Adali, T., Pearlson, G.D., Pekar, J.J., 2001. Spatial and temporal independent component analysis of functional MRI data containing a pair of task-related waveforms. Hum. Brain Mapp. 13, 43–53.

Cox, R.W., 1996. AFNI software for analysis and visualization of functional magnetic resonance neuroimages. Comput. Biomed. Res. 29, 162–173.

Cramer, S.C., Finklestein, S.P., Schaechter, J.D., Bush, G., Rosen, B.R., 1999. Activation of distinct motor cortex regions during ipsilateral and contralateral finger movements. J. Neurophysiol. 81, 383–387.

Doyon, J., Song, A.W., Karni, A., Lalonde, F., Adams, M.M., Ungerleider, L.G., 2002. Experience-dependent changes in cerebellar contributions to motor sequence learning. Proc. Natl. Acad. Sci. U. S. A. 99, 1017–1022.

Duann, J.R., Jung, T.P., Kuo, W.J., Yeh, T.C., Makeig, S., Hsieh, J.C., Sejnowski, J.T., 2002. Single-trial variability in event-related BOLD signals. NeuroImage 15, 823–835.

Filzmoser, P., Baumgartner, R., Moser, E., 1999. A hierarchical clustering method for analyzing functional MR images. Magn. Reson. Imaging 17, 817–826.

Friston, K.J., 1996. Statistical parametric mapping and other analyses of functional imaging data. In: Toga, A.W., Mazziotta, J.C. (Eds.), Brain Mapping: the Methods. Academic Press, San Diego, CA, pp. 363–396.

Goutte, C., Toft, P., Rostrup, E., Nielsen, F., Hansen, L.K., 1999. On clustering fMRI time series. NeuroImage 9, 298–310.

Greicius, M.D., Krasnow, B., Reiss, A.L., Menon, V., 2003. Functional connectivity in the resting brain: a network analysis of the default mode hypothesis. Proc. Natl. Acad. Sci. U. S. A. 100, 253–258.

Hamzei, F., Dettmers, C., Rzanny, R., Liepert, J., Buchel, C., Weiller, C., 2002. Reduction of excitability ("inhibition") in the ipsilateral primary motor cortex is mirrored by fMRI signal decreases. NeuroImage 17, 490–496.

Hansen, L.K., Larsen, J., Nielsen, F.A., Strother, S.C., Rostrup, E., Savoy, R., Lange, N., Sidtis, J., Svarer, C., Paulson, O.B., 1999. Generalizable patterns in neuroimaging: how many principal components? NeuroImage 9, 534–544.

Kendall, M., Gibbons, J.D., 1990. Rank Correlation Methods. Oxford Univ. Press, Oxford.

Lai, S.H., Fang, M., 1999. A novel local PCA-based method for detecting activation signals in fMRI. Magn. Reson. Imaging 17, 827–836.

Lu, Y.L., Jiang, T.Z., Zang, Y.F., 2003. Region growing method for the analysis of fMRI data. NeuroImage 20, 455–465.

Mazoyer, B., Zago, L., Mellet, E., Bricogne, S., Etard, O., Houde, O., Crivello, F., Joliot, M., Petit, L., Tzourio-Mazoyer, N., 2001. Cortical networks for working memory and executive functions sustain the conscious resting state in man. Brain Res. Bull. 54, 287–298.

McKeown, M.J., Makeig, S., Brown, G.G., Jung, T.P., Kindermann, S.S., Bell, A.J., Sejnowski, T.J., 1998. Analysis of fMRI data by blind separation into independent spatial components. Hum. Brain Mapp. 6, 160–188.

Moritz, C.H., Meyerand, M.E., Cordes, D., Haughton, V.M., 2000. Functional MR imaging activation after finger tapping has a shorter duration in the basal ganglia than the sensorimotor cortex. Am. J. Neuroradiol. 21, 1228–1234.

Ngan, S.C., Hu, X., 1999. Analysis of functional magnetic resonance imaging data using self-organizing mapping with spatial connectivity. Magn. Reson. Med. 41, 939–946.

Ogawa, S., Lee, T.M., Kay, A.R., Tank, D.W., 1990. Brain magnetic resonance imaging with contrast dependent on blood oxygenation. Proc. Natl. Acad. Sci. U. S. A. 87, 9868–9872.

Raichle, M.E., MacLeod, A.M., Snyder, A.Z., Powers, W.J., Gusnard, D.A., Shulman, G.L., 1997. A default mode of brain function. Proc. Natl. Acad. Sci. U. S. A. 98, 676–682.

Richter, W., Ugurbil, K., Georgopoulos, A., Kim, S.G., 1997. Time-resolved fMRI of mental rotation. NeuroReport 8, 3697–3702.

Salmelin, R., Forss, N., Knuutila, J., Hari, R., 1995. Bilateral activation of the human somatomotor cortex by distal hand movements. Electroencephalogr. Clin. Neurophysiol. 95, 444–452.

Shulman, G.L., Fiez, J.A., Corbetta, M., Buckner, R.L., Miezin, F.M., Raichle, M.E., Petersen, S.E., 1997. Common blood flow changes across visual tasks: II. Decreases in cerebral cortex. J. Cogn. Neurosci. 9, 648–663.

Smith, S., 2002. Fast robust automated brain extraction. Hum. Brain Mapp. 17, 143–155.

Talairach, J., Tournoux, P., 1988. A Coplanar Stereotactic Atlas of the Human Brain. Thieme, Stuttgart.

Urbano, A., Babiloni, C., Onorati, P., Carducci, F., Ambrosini, A., Fattorini, L., Babiloni, F., 1998. Responses of human primary sensorimotor and supplementary motor areas to internally triggered unilateral and simultaneous bilateral one-digit movements. A high-resolution EEG study. Eur. J. Neurosci. 10, 765–770.

Ziemann, U., Hallett, M., 2001. Hemispheric asymmetry of ipsilateral motor cortex activation during unimanual motor tasks: further evidence for motor dominance. Clin. Neurophysiol. 112, 107–113.